Applied Physics Express

The Japan Society of Applied Physics

LETTER • **OPEN ACCESS**

Sub-two-cycle intense pulse generation based on two-stage hollow-core fiber compression using an ytterbium amplifier

To cite this article: Nobuhisa Ishii and Ryuji Itakura 2024 *Appl. Phys. Express* **17** 042006

View the article online for updates and enhancements.

You may also like

- Tools for numerical modelling of nonlinear propagation in hollow capillary fibres and their application
Aurora Crego, Julio San Roman and Enrique Conejero Jarque
- Photovoltammetry of *p*-Phenylenediamine Mediated by Hexacyanoferrate Immobilized on CdS-Graphene Nanocomposites
Jinnan Wu, Yuhan Zhu, Kai Yan et al.
- Double-end low-loss coupling of anti-resonant hollow-core fibers with solid-core single-mode fibers by tapering technique
Hao Li, Wei Huang, Zefeng Wang et al.

This content was downloaded from IP address 3.144.230.82 on 07/05/2024 at 16:12

OPEN ACCESS

Applied Physics Express 17, 042006 (2024) LETTER

https://doi.org/10.35848/1882-0786/ad3cb5

Sub-two-cycle intense pulse generation based on two-stage hollow-core fiber compression using an ytterbium amplifier

Nobuhisa Ishii* and Ryuji Itakura

Kansai Institute for Photon Science, National Institutes for Quantum Science and Technology (QST), Kizugawa, Kyoto, 619-0215, Japan

*E-mail: ishii.nobuhisa@qst.go.jp

Received February 14, 2024; revised March 27, 2024; accepted April 8, 2024; published online April 26, 2024

We demonstrate the generation of sub-two-cycle intense laser pulses based on two-stage hollow-core fiber (HCF) compression in a compact setup (footprint of 0.65 m × 2.85 m) using a commercial Yb:KGW regenerative amplifier. Spectrally broadened laser pulses with an output power of 7.2 W from the second HCF stage are compressed down to 6.6 fs (1.9 cycles at 1030 nm) using a pair of chirp mirrors and a pair of wedges with an efficiency of 86%, leading to a compressed output of 6.2 W. A pulse-to-pulse energy stability of 0.17% is measured for 10 min.
© 2024 The Author(s). Published on behalf of The Japan Society of Applied Physics by IOP Publishing Ltd

For decades, ultrashort laser technology based on Ti:sapphire lasers[1] has constituted an essential part in ultrafast laser science.[2] Chirped-pulse amplification (CPA) technology[3] has been successfully applied to the generation of intense ultrashort laser pulses with a temporal duration of several tens of femtoseconds thanks to extremely broad gain in Ti:sapphire amplifiers. Post-pulse nonlinear compression of Ti:sapphire laser pulses, which is based on spectral broadenings such as hollow-core fiber (HCF) pulse compression followed by chirp-mirror-based dispersion compensation,[4] provides the generation of intense few-cycle laser pulses that is an essential part for the generation of attosecond pulses[5,6] via high harmonic generation in noble gases.[7] However, the Ti:sapphire laser technology has its shortcomings such as low laser power of a 10 W level due to the thermal problem associated with the low quantum efficiency and its complicated laser system requiring expensive green lasers for pumping a Ti:sapphire amplifier.

Recent advance in ytterbium (Yb)-based lasers has shown unprecedented power scalability up to a kilowatt-level, nearly two orders of magnitude higher than that of Ti:sapphire lasers. In addition, a low-cost diode laser can be used as a pump source, reducing the cost of Yb lasers and increasing its reliability and stability.

High-power output from Yb lasers enables high-repetition-rate ($\gg$1 kHz) pulsed laser operation, making them attractive in a wide variety of scientific and industrial applications such as laser machining,[8] attosecond photoelectron spectroscopy with gaseous[9] and solid[10] targets and photoelectron photo-ion coincidence spectroscopy such as cold target recoil-ion momentum spectroscopy.[11] However, long temporal duration of the output pulses from Yb lasers, which ranges from hundreds of femtoseconds to few picoseconds, makes the generation of few-cycle pulses extremely challenging, limiting Yb lasers to be a workhorse in attosecond science.

To overcome this limitation, a variety of nonlinear pulse compression methods have been proposed and experimentally demonstrated.[12,13] Multiple-plate pulse compression (MPPC)[14] has been realized to compress femtosecond pulses with intermediate pulse energies on the order of $\sim$100 μJ, which is too low for HCF-based pulse compression and too high for supercontinuum generation from a single filament in solid. MPPC has been applied to the generation of few-cycle pulses using Yb:KGW lasers with an output energy of less than 1 mJ.[15–17] Millijoule-class intense femtosecond pulses have been demonstrated by MPPC at a low repetition rate of 1 kHz,[16] because the generation of mJ-class pulses at multi-kHz repetition rates has been severely limited by the onset of plasma generated in air.[18] This limitation has been solved by using a helium-filled gas cell around the focus of laser pulses prior to a multi-plate section.[19]

Multi-pass nonlinear pulse compression schemes have been demonstrated using solid[20,21] and gas[22] as nonlinear media to shorten a long pulses with relatively low pulse energy. Recently, the generation of 6.9 fs, 0.78 mJ pulses at 500 kHz has been achieved by using a silver mirror-based multi-pass cell.[23] Hädrich et al., demonstrated two-stage multi-pass-cell compression of a Yb fiber-based CPA system to deliver sub-two-cycle (5.8 fs), 1.07 mJ, carrier-envelope-phase-stable laser pulses at 100 kHz.[24] Four-pass pulse compression in argon has been shown by adopting intermediate pulse compression using chirp mirrors that decreases substantially the required number of pass to generate 3.1 fs, 0.98 mJ pulses at 4 kHz.[25]

Nonlinear propagation in a gas-filled HCF has been widely applied to the pulse compression of Yb lasers.[26–34] The generation of few-cycle pulses based on HCF has been achieved by employing two-stage HCF compression,[26,31] single-stage long (>3 m) HCFs,[29,32,33] or a highly pressurized (27 bar) neon-filled HCF.[34] The two-stage approach is easily implemented in a compact optical table. However, so far, the two-stage approach has been realized with a low throughput of less than 40%.

In this work, based on two-stage pulse compression using large-inner-core HCFs with much higher throughput, we report the generation of intense sub-two-cycle pulses around 850–1180 nm at 10% of the peak intensity based on the pulse compression of the output pulses from a commercial Yb regenerative amplifier (10 W, 1 mJ, 184 fs). The output pulses with a power of 7.2 W from the second HCF stage are compressed down to 6.6 fs (1.9 cycles at 1030 nm) by using a pair of chirp mirrors and fused silica wedges with an efficiency of 86%, leading to an output power of 6.2 W at 10 kHz repetition rate.

A schematic of the experimental setup is shown in Fig. 1. The output pulses (pulse energy: 1 mJ, temporal duration:

Content from this work may be used under the terms of the Creative Commons Attribution 4.0 license. Any further distribution of this work must maintain attribution to the author(s) and the title of the work, journal citation and DOI.
© 2024 The Author(s). Published on behalf of The Japan Society of Applied Physics by IOP Publishing Ltd

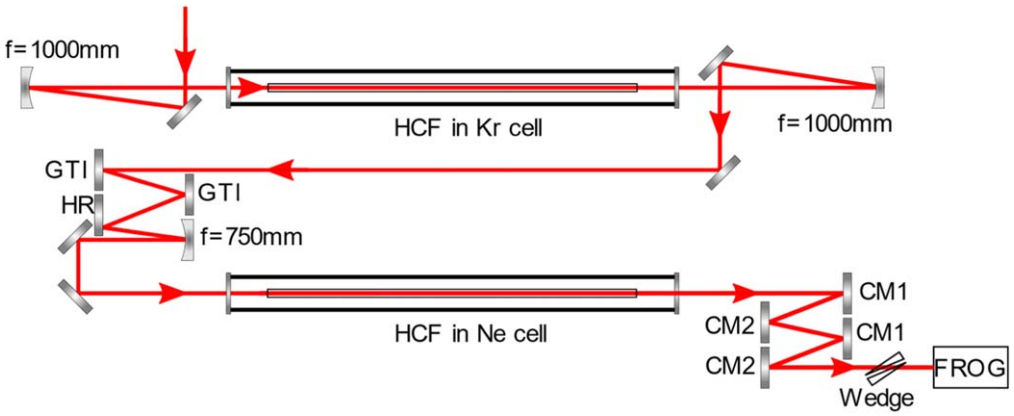

Fig. 1. Schematic of the two-stage HCF pulse compression. HCF, hollow-core fiber; GTI, Gires–Tournois Interferometer Mirror (GDD = $-200\,\mathrm{fs}^2$); HR, High reflector (AOI = 0 deg); CM1 and CM2, Mirrors of the chirp-mirror pair (GDD = $-60\,\mathrm{fs}^2$); Wedge, fused silica wedge pair; FROG, frequency-resolved optical gating apparatus.

184 fs, repetition rate: 10 kHz, central wavelength: 1033 nm) of a commercial Yb:KGW laser (Pharos PH2-SP-10 W-1 mJ-200 kHz, LIGHT CONVERSION) are focused by a concave mirror (f = 1000 mm) into a 1 m long fused silica HCF (Nakahara Opto-Electronics Laboratories, Inc.) with an inner-core diameter of 400 μm. The HCF with an outer diameter of 3 mm is kept straight in an aluminum V-shaped groove placed in a gas cell filled with a 1 bar of krypton. The entrance and exit windows of all gas cells used in this experiment are made of 1 mm thick fused silica with appropriate anti-reflection coating.

Contrast to a smaller ($\leqq$250 μm)-inner-diameter HCF customary chosen in many works,[26,27,31,34] we employ a relatively large inner-core HCF to ensure high throughput of the laser pulses as well as to, more importantly, avoid excess plasma effect that severely deteriorates the stability of output pulses from a HCF.[18] As a consequence, the larger-inner-core-diameter HCF does not provide high pulse compression ratio, which is typically more than several dozens in the case with a smaller-inner-core-diameter HCF. Therefore, we employ the two-stage HCF pulse compression scheme to compensate for the low pulse compression ratio.

At the focal point in the first HCF stage, the beam diameter (full width at $1/e^2$) is measured to be ~240 μm that is closed to a theoretically optimized value of 260 μm,[27,35] ensuring reliable operation with a fundamental mode of the HCF as well as high transmission throughput simultaneously.

The output pulses with a power of 8.8 W from the first HCF stage are re-collimated by a concave mirror with a focal distance of 1 m. The output laser pulses from the first stage are spectrally broadened up to 175 nm wide from 925 to 1100 nm at 10% of the peak intensity measured with an InGaAs-based infrared optical multichannel analyzer (NIR-Quest 512-1.7, Ocean Insight) as shown by the black dashed curve in Fig. 2(c).

The spectrally broadened pulses are checked to be compressible by Gires–Tounois-Interferometer (GTI) mirrors (#12–328, designed GDD = $-200\,\mathrm{fs}^2$ from 950 to 1120 nm, Edmund) and characterized by a second-harmonic-generation (SHG) frequency-resolved optical gating (FROG) apparatus. A temporal duration of 17.9 fs retrieved with a FROG reconstruction error of 0.40% over 256 × 256 grids has been achieved by three bounces on the GTI mirrors, while the transform-limited pulse duration is 17.2 fs. The results of the pulse characterization are summarized in Fig. 2.

Although the spectrally broadened pulses in the first stage are fully compressible close to the transform-limited pulse duration by three bounces on the GTI mirrors, we employ a partially compressed pulse with a duration of ~80 fs after two bounces on the GTI mirrors as an input pulse to the second HCF stage. This is because even helium filled in the second HCF stage with an inner-core diameter of 400 μm has been heavily ionized by the fully compressed pulses with a temporal duration of less than 20 fs. As a result of heavy ionization, dense plasma mainly formed near the entrance of the second HCF deteriorates the throughput of the pulse energy, the spectral phase of the broadened pulses and the stability of the output pulses.

The partially compressed pulses with a duration of ~80 fs are focused by a concave mirror (f = 750 mm) into a 1 m long fused silica HCF with an inner-core diameter of 400 μm similar to that used in the first stage. The HCF supported by a V-shaped groove is placed in a gas cell filled with a 2.2 bar of neon. At the focal point in the second HCF stage, the beam diameter (full width at $1/e^2$) is measured to be ~300 μm that is closed to a theoretically optimized value of 260 μm. The green and red dashed curves in Fig. 3(c) show blue and red parts of the spectrum of the broadened pulses in the second stage, which are measured with a silicon-based visible-to-infrared optical multichannel analyzer (USB4000, Ocean Optics) and the infrared optical multichannel analyzer, respectively. The output power of the spectrally broadened pulses is measured to be 7.2 W.

The broadened pulses are compressed by two bounces on each of a pair of chirp mirrors (#14–674, designed GDD = $-60\,\mathrm{fs}^2$ from 650 to 1350 nm, Edmund) and the residual dispersion is compensated for by a pair of fused silica wedges (23RQ12-02, Newport). The throughput of the chirp mirror pairs and the wedges is measured to be 86%, leading to an output power of the compressed pulses to be 6.2 W. Figure 3 summarizes the results of the characterization of the compressed pulses by the SHG-FROG apparatus. The temporal duration of the compressed pulses is retrieved to be 6.6 fs (1.9 cycles at 1030 nm) with a FROG reconstruction error of 0.70% over 512 × 512 grids, while the duration of the transform-limited pulses is 6.4 fs.

© 2024 The Author(s). Published on behalf of The Japan Society of Applied Physics by IOP Publishing Ltd

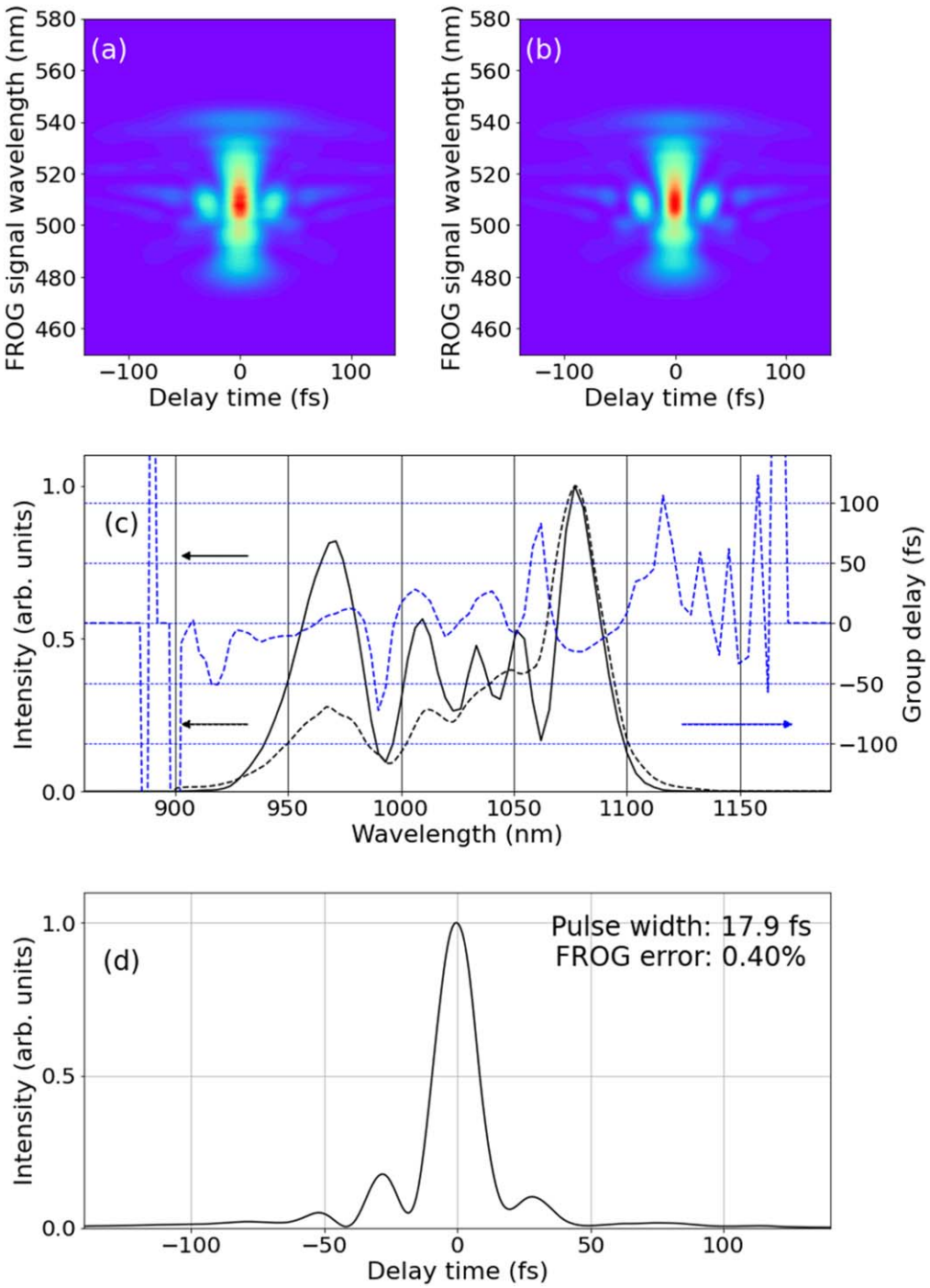

Fig. 2. Summary of SHG-FROG results in the first HCF compression stage. (a) Measured FROG trace. (b) Reconstructed FROG trace (the FROG error is 0.40% over 256 × 256 grids), (c) (i) spectral intensity measured with an InGaAs-based infrared optical multichannel analyzer (NIR-Quest 512-1.7, Ocean Insight, black dashed curve), (ii) spectral intensity retrieved from the FROG measurement (black solid curve), and (iii) group delay retrieved from the FROG measurement (blue dashed curve). (d) Retrieved temporal profile with a pulse duration of 17.9 fs (full width at half maximum). Note that the temporal width of the transform-limited pulse assuming a flat phase is 17.2 fs (full width at half maximum).

We also demonstrate the characterization of the spatial profile and the energy stability in the two-stage HCF compression. As shown in Fig. 4, the spatial profile of the output pulses has been measured 1.0 m downstream the exit of the second HCF by an InGaAs-based infrared camera (Goldeye G-008 TEC1, ALLIED Vision Technologies GmbH). The smooth gaussian-like profile ensures the reliable operation of our compressor in the fundamental mode of the HCF.

The shot-to-shot stability of the output pulse energy from the second HCF has been measured by recoding and analyzing the signals from an InGaAs-based photodiode with a fast oscilloscope. The root-mean-square (RMS) error of the pulse-to-pulse energies divided by their mean value is measured to be 0.17% for 10 min, indicating that our scheme does not suffer from plasma instability in the HCFs. The long-term stability of the output power from the second HCF has been measured to be 0.13% (RMS error) for 31.5 h. Note

© 2024 The Author(s). Published on behalf of The Japan Society of Applied Physics by IOP Publishing Ltd

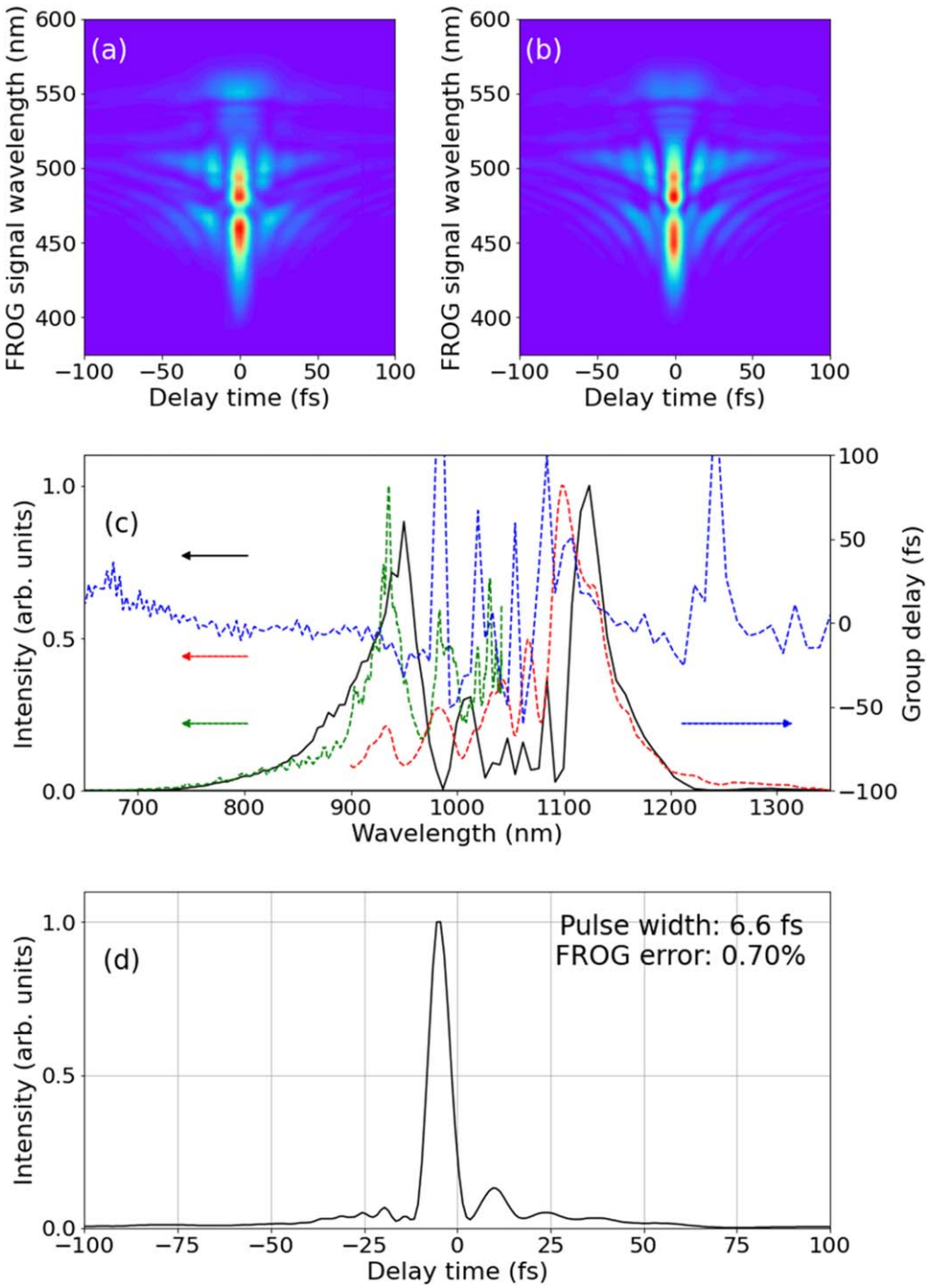

Fig. 3. Summary of SHG-FROG results in the second HCF compression stage. (a) Measured FROG trace. (b) Reconstructed FROG trace (the FROG error is 0.70% over 512 × 512 grids), (c) (i) spectral intensities measured in the visible-to-infrared part (green dashed curve) and in the infrared part (red dashed curve), (ii) spectral intensity retrieved from the FROG measurement (black solid curve), and (iii) group delay retrieved from the FROG measurement (blue dashed curve). (d) Retrieved temporal profile with a pulse duration of 6.6 fs (full width at half maximum). Note that the temporal width of the transform-limited pulse assuming a flat phase is 6.4 fs (full width at half maximum).

that the long-term stability is measured with a power meter, which averages out the output fluctuations for a few seconds. Both stability measurements have been performed with pointing stabilizers installed at both HCF stages to compensate a slow drift (∼1 s) of the beam pointing.

In summary, we have demonstrated the generation of sub-two-cycle intense pulses based on two-stage HCF pulse compression using a commercial Yb:KGW amplifier. More than 25 times compression has been achieved by using krypton- and neon-filled HCFs with dispersion compensation by chirp mirrors and fused silica wedges. The spectrally broadened pulses from the first and second HCF stages are proven to be compressible down to 17.9 fs and 6.6 fs (1.9 cycles at 1030 nm), respectively.

By employing large inner-core HCFs, we have achieved high throughputs of 88% and 82% in the first and second HCF stages, respectively, yielding a final output power of 6.2 W after the final pulse compression. The total efficiency of 62% in the two-stage HCF pulse compression is the highest efficiency, to the best of our knowledge. This high efficiency is realized by adopting large-inner-core-diameter HCFs. Our two-stage pulse compression system is assembled in a relatively compact setup

© 2024 The Author(s). Published on behalf of The Japan Society of Applied Physics by IOP Publishing Ltd

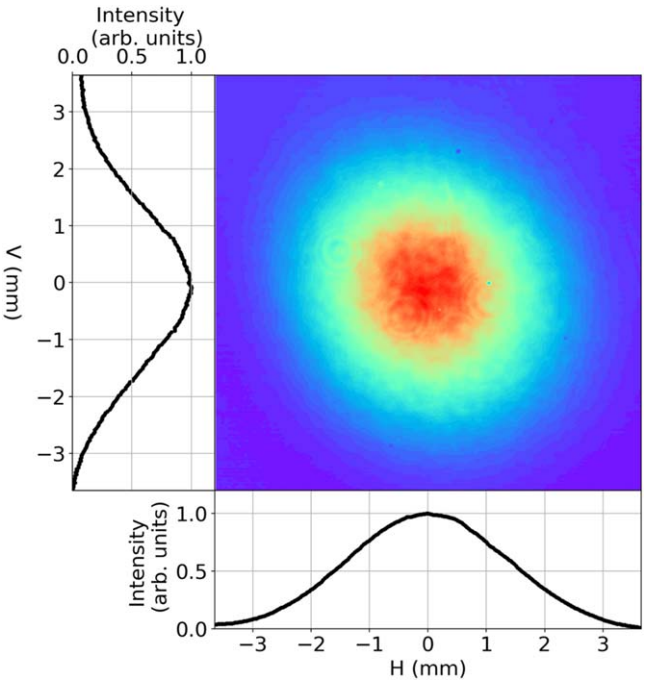

Fig. 4. Beam profile measured 1.0 m downstream the exit of the second HCF, confirming the operation in the fundamental mode.

(footprint of 0.65 m × 2.85 m). The stabilities of the shot-to-shot pulse energy and the long-term output power have been measured to be 0.17% (RMS error) for 10 minuites and 0.13% (RMS error) for 31.5 h, respectively.

Combined our results with the stabilization of the carrier envelope phase of Yb:KGW amplifiers, our demonstration opens a practical way toward a reliable compact high-repetition-rate light source for the exploration of attosecond science.

Acknowledgments This study was partially supported by JSPS KAKENHI Grant No. JP23H01108 and by QST President's Strategic Grant (Creative Research).

ORCID iDs Nobuhisa Ishii https://orcid.org/0000-0001-7181-3357 Ryuji Itakura https://orcid.org/0000-0003-0508-4760

1) P. F. Moulton, J. Opt. Soc. Am. B **3**, 125 (1986).
2) A. H. Zewail, *Femtochemistry* (World Scientific, Singapore, 1994).
3) D. Strickland and G. Mourou, Opt. Commun. **56**, 219 (1985).
4) M. Nisoli, S. De Silvestri, O. Svelto, R. Szipöcs, K. Ferencz, C. Spielmann, S. Sartania, and F. Krausz, Opt. Lett. **22**, 522 (1997).
5) P. M. Paul, E. S. Toma, P. Breger, G. Mullot, F. Aug´e, P. Balcou, H. G. Muller, and P. Agostini, Science **292**, 1689 (2001).
6) M. Hentschel, R. Kienberger, C. Spielmann, G. A. Reider, N. Milosevic, T. Brabec, P. Corkum, U. Heinzmann, M. Drescher, and F. Krausz, Nature **414**, 509 (2001).
7) M. Ferray, A. L'Huillier, X. F. Li, L. A. Lompré, G. Mainfray, and C. Manus, J. Phys. B: At. Mol. Opt. Phys. **21**, L31 (1988).
8) C. Kerse et al., Nature **537**, 84 (2016).
9) R. Kienberger et al., Nature **427**, 817 (2004).
10) A. L. Cavalieri et al., Nature **449**, 1029 (2007).
11) R. Dörner, V. Mergel, O. Jagutzki, L. Spielberger, J. Ullrich, R. Moshammer, and H. Schmidt-Böcking, Phys. Rep. **330**, 95 (2000).
12) T. Nagy, P. Simon, and L. Veisz, Adv. Phys.: X **6**, 1845795 (2020).
13) A.-L. Viotti, M. Seidel, E. Escoto, S. Rajhans, W. P. Leemans, I. Hartl, and C. M. Heyl, Optica **9**, 197 (2022).
14) C.-H. Lu, Y.-J. Tsou, H.-Y. Chen, B.-H. Chen, Y.-C. Cheng, S.-D. Yang, M.-C. Chen, C.-C. Hsu, and A. H. Kung, Optica **1**, 400 (2014).
15) N. Ishii, P. Xia, T. Kanai, and J. Itatani, Opt. Express **27**, 11447 (2019).
16) C.-H. Lu, W.-H. Wu, S.-H. Kuo, J.-Y. Guo, M.-C. Chen, S.-D. Yang, and A. H. Kung, Opt. Express **27**, 15638 (2019).
17) T. Okamoto, Y. Kunihashi, Y. Shinohara, H. Sanada, M.-C. Chen, and K. Oguri, Opt. Lett. **48**, 2579 (2023).
18) Y.-H. Cheng, J. K. Wahlstrand, N. Jhajj, and H. M. Milchberg, Opt. Express **21**, 4740 (2013).
19) M. Tsubouchi, N. Ishii, Y. Kagotani, R. Shimizu, T. Fujita, M. Adachi, and R. Itakura, Opt. Express **31**, 6890 (2023).
20) J. Schulte, T. Sartorius, J. Weitenberg, A. Vernaleken, and P. Russbueldt, Opt. Lett. **41**, 4511 (2016).
21) J. Weitenberg, A. Vernaleken, J. Schulte, A. Ozawa, T. Sartorius, V. Pervak, H.-D. Hoffmann, T. Udem, P. Russbüldt, and T. W. Hänsch, Opt. Express **25**, 20502 (2017).
22) L. Lavenu, M. Natile, F. Guichard, Y. Zaouter, X. Delen, M. Hanna, E. Mottay, and P. Georges, Opt. Lett. **43**, 2252 (2018).
23) M. Müller, J. Buldt, H. Stark, C. Grebing, and J. Limpert, Opt. Lett. **46**, 2678 (2021).
24) S. Hädrich et al., Opt. Lett. **47**, 1537 (2022).
25) M.-S. Tsai, A.-Y. Liang, C.-L. Tsai, P.-W. Lai, M.-W. Lin, and M.-C. Chen, Sci. Adv. **8**, eabo1945 (2022).
26) J. Rothhardt, S. Hädrich, A. Klenke, S. Demmler, A. Hoffmann, T. Gotschall, T. Eidam, M. Krebs, J. Limpert, and A. Tünnermann, Opt. Lett. **39**, 5224 (2014).
27) X. Guo, S. Tokita, K. Yoshii, H. Nishioka, and J. Kawanaka, Opt. Express **25**, 21171 (2017).
28) S.-Z. A. Lo, L. Wang, and Z.-H. Loh, Appl. Opt. **57**, 4659 (2018).
29) Y.-G. Jeong et al., Sci. Rep. **8**, 11794 (2018).
30) J. E. Beetar, F. Rivas, S. Gholam-Mirzaei, Y. Liu, and M. Chini, J. Opt. Soc. Am. B **36**, A33 (2019).
31) R. Klas, W. Eschen, A. Kirsche, J. Rothhardt, and J. Limpert, Opt. Express **28**, 6188 (2020).
32) J. E. Beetar et al., Sci. Adv. **6**, eabb5375 (2020).
33) R. Feng, Y. Peng, Y. Li, W. Li, J. Qian, L. Shen, Y. Leng, and R. Li, Opt. Laser Technol. **154**, 108279 (2022).
34) Z. Pi, H. Y. Kim, and E. Goulielmakis, Opt. Lett. **47**, 5865 (2022).
35) C. Vozzi, M. Nisoli, G. Sansone, S. Stagira, and S. De Silvestri, Appl. Phys. B **80**, 285 (2005).

© 2024 The Author(s). Published on behalf of The Japan Society of Applied Physics by IOP Publishing Ltd